Journal of Polymers and the Environment (2020) 28:1465–1474
https://doi.org/10.1007/s10924-020-01695-x

ORIGINAL PAPER

Extraction of High Crystalline Nanocellulose from Biorenewable Sources of Vietnamese Agricultural Wastes

Vu Nang An[1,2] · Ha Thuc Chi Nhan[1,2] · Tran Duy Tap[1,2] · Tran Thi Thanh Van[1,2] · Pham Van Viet[1,2] · Le Van Hieu[1,2]

Published online: 14 March 2020

Abstract

Cellulose nanocrystals (CNCs) is one of the interesting materials attracting many researchers from the decades, especially when they are extracted from natural biomass resources. This study focuses on the isolation of CNCs with high crystallinity from Vietnamese agricultural wastes (*Nypa Fruticans* trunk, coconut husk fiber, and rice husk). CNCs were extracted from the above natural sources by a three-step process including formic/peroxyformic acid pre-treatment, hydrogen peroxide/sodium hydroxide treatment, and a hydrolysis disintegration process. The structure and thermal property of obtained materials after each stage of treatments were characterized by XRD, TGA, TEM, and FT-IR analysis. TEM observation has showed the CNCs with high aspect ratio in shape of 200–500 nm in length and 10–15 nm in width. FT-IR results indicated that lignin was completely removed from the samples during chemical treatment. The high crystalline index (nearly 80%) and improved thermal stability of the CNCs nanofibers indicate its various potential applications.

Keywords *Nypa Fruticans* trunk (NFT) · Coconut husk fiber (CHF) · Rice husk (RH) · Biomass · Crystalline nanocellulose

Introduction

Over the past decades, nanotechnology has been emerging as an attractive phenomenon in all over the world. It has not only opened a great deal of new prospects but also attributed to facilitate the development of variety of different fields, such as medicine, construction, dentistry, textiles, electronic components, food packaging. One of nanoscale materials recently drawing growing attention of scientists is cellulose nanocrystals (CNCs) which is known as a potential reinforcing component for synthesis of high performance nanocomposite thanks to its distinctive properties such as biodegradability, renewability, non-toxic, low density, high strength and modulus, large specific surface area, and reactive surface [1, 2]. However, this nanosized polysaccharide material is naturally embedded in the plant cell walls with hierarchical structures and complex compositions. The inner hemicellulose plays as cement which links the strong outermost lignin layers to the core cellulose which is the main obstacle for direct extraction of nanocellulose.

In literatures, CNCs is usually extracted from the lignocellulosic materials by several methods, including chemical treatments (acid hydrolysis, TEMPO-mediated oxidation hydrolysis treatment) [3–5], mechanical treatments (cryocrushing, grinding, high-intensity ultrasonication, and twin screw extrusion) [6, 7], biological treatments (enzyme-assisted hydrolysis), and even the integration of aforementioned process [8–10]. The properties of nanocellulose materials depend mostly on the sources of cellulose, pretreatment, isolation method, and conditions [11–13]. Recently, the CNCs can be collected from a variety of renewable organic materials like wood, cotton, bacterial cellulose, agricultural crops [14]. In these biosources, wood, hemp, cotton, linen, etc. have been used by our society as engineering materials for thousands of years and today their utilization continues confirming by the enormity of the world-wide industries in forest products, paper, textiles, etc.. However, because of the environmental pollution concerns as well as the diminishing forest, non-wooden cellulosic materials became exploiting [15]. Million tons of bio-waste from food processing or agricultural processing (by-products) are produced every month

✉ Ha Thuc Chi Nhan
htcnhan@hcmus.edu.vn

✉ Le Van Hieu
lvhieu@hcmus.edu.vn

[1] Faculty of Materials Science and Technology, University of Science, VNU–HCMC, Ho Chi Minh City, Vietnam

[2] Vietnam National University Ho Chi Minh City, Ho Chi Minh City, Vietnam

such as grain straw, coconut husk fiber, grape skin, banana rachis, garlic peel, soy hulls, sugarcane bagasse, etc. [12, 15–20] turned them into brilliant candidates for estimation of economic potential goal of large quantities of cellulose every year. Some exceptional properties of lignocellulose derived from bio-waste or by-products can be mentioned as low cost, hollow cellular structure, abundance, biodegradability, renewability [21].

In Vietnam, some by-products with high potential for the extraction of renewable cellulosic resources are *Nypa Fruticans* trunk, coconut husk fiber, and rice husk. In fact, as the third largest rice exporter in the world, every year Vietnam produces over 40 million tons of grain of rice [22, 23]. The amount of rice husk (RH) is about 20% of the grain, so about 9 million tons of rice husks are released into the environment each year, which is a huge amount of waste causing the pollution of environment if they are not well treated. Like *Nypa Fruticans* trunk (NFT) and coconut husk fiber (CHF), RH is often considered as low value material and used mainly in agriculture, fertilizer, animal feed, combustion byproducts, and sometimes for livestock [23].

In this study, the main objective was to valorize agro-industrial solid residues for the obtaining of value-added CNCs. Here, we have conducted a systematic study of the CNCs synthesis from three renewable sources of agricultural products in Vietnam, especially using formic / peroxyformic acid in extract process. Moreover, the research achieved interesting results in case of the material source of *Nypa Fruticans* trunk which is a very typical tree category in the southwest wetlands of Vietnam.

According to our knowledge, the preparation of CNCs from NFT, which has not been reported before, expected bringing more interesting properties for variety of applications. The potential CNCs extracted from NFT, CHF, and RH was comprehensively investigated in terms of structure, morphology, crystallinity and thermal degradation.

Experimental

Materials

Nypa Fruticans trunk (NFT) was obtained from muddy areas along the riverside in Ben Tre, whereas rice husk (RH) was collected from local fields in Cu Chi, Ho Chi Minh city. Coconut husk fiber (CHF) was picked up in Ben Tre. All raw cellulose bulk was derived from South of Vietnam. Sodium hydroxide (NaOH, 96%) was purchased from Guangdong Guanghua Sci-Tech Co., Ltd., China. Formic acid (HCOOH, 90%), hydrogen peroxide (H_2O_2, 30%), and sulfuric acid (H_2SO_4, 98%) were procured from Xilong Scientific Co.,Ltd, China.

Chemical Analysis and Isolation of Cellulose

Cellulose was extracted from NFT, RH, and CHF by following procedure: First of all, the raw cellulose bulk of NFT was peeled off and cut into chunks around 30 cm in length and 1 cm in depth. These chunks of NFT had been then laminated by a rolling machine before dried and split into fibers. Each biomass (the dried fibers of NFT, RH, and CHF) was ground to fine powder. Fifty grams of dried biomass powder were stirred well in 1000 ml of distilled water at 100 °C for 2 h to remove impurities and aqueous soluble substances; they were then cooled to room temperature and filtered by filter paper. This process was conducted twice and the final bulk celluloses were then dried in an air oven at 70 °C for 8 h. Twenty grams of the pretreated biomass powder were dispersed into HCOOH 90% (1:10 w/v) at 100 °C for 2 h under magnetic agitator in circulation system, then filtered by filter paper and washed the residue with pure HCOOH acid and warm distilled water to break the –O–4 linkages of hemicellulose and take it onto fiber surface which created an easy premise for the following steps as well as dissolve the remnants of impurities. To remove hemicellulose, the samples after pre-treated with acid were dissolved into PFA (a mixed solvent of formic acid, hydrogen peroxide, and distilled water with the ratio was 90:4:6% w/w, respectively) and stirred well at 80 °C for 2 h, then filtered and washed with formic acid (80%) and distilled water, respectively. Next, the fiber was bleached at pH 11 by adding the required amount of NaOH to the suspension of unbleached fiber and H_2O_2 with fiber to H_2O_2 ratio of 1:1 w/w. Bleaching experiments were carried out under magnetic stirring circulation system at 80 °C for 1 h, then filtered and rinsed several times to get rid of lignin and hemicelluloses, and finally gain white cellulose in slurry. The bleaching step was conducted two times to ensure these additional contents were completely removed from cellulose fibers.

Isolation of Cellulose Nanocrystals (CNCs)

CNCs were extracted from cellulose derived from NFT, RH, and CHF using an acid hydrolysis method. The white cellulose was hydrolyzed using sulfuric acid solution (64%) with the ratio of 1:15 at 45 °C for 30 min with strong agitation in circulation system. To avoid aggregation and sedimentation of particles due to Van Der Waals linking force, the suspension was sonicated, using a high intensity ultrasonic processor (UP200St, Hielscher) during 10 min to obtain nano-scale crystal cellulose. The total efficiency of nanocellulose synthesis is calculated by the below equation:

$$\text{Yield}\% = \frac{\textit{Dry weight of nanocellulose}\,(g)}{\textit{Dry weight of crude fiber}\,(g)} \times 100$$

Characterization of Cellulose

Fourier Transformed Infrared Spectroscopy

Any varieties in functional groups of each stage of treatment were recorded on a Fourier transform infrared (FT-IR) (TENSOR 27, Bruker, Germany). The samples were dried, ground with KBr (1:100 w/w) and pressed into transparent pellets. The IR spectra of the pellets were recorded at a wavenumber range of 400÷4000 cm^{-1}.

Transmission Electron Microscopy

Transmission electron microscopy (TEM) (model Japan JEOL JEM-1400) was used to estimate the dimensions of CNCs isolated from NFT, RH, and CHF. A drop of diluted suspension was deposited onto glow-discharged carbon-coated TEM grids and the excess liquid was removed by blotting with a filter paper. The samples were then dried at ambient temperature before TEM observation was conducted with an accelerating voltage of 100 kV.

X-ray Diffraction (XRD)

XRD patterns of the fibers at different stages were measured by using D2 PHASER X-ray powder diffractometer (Bruker, Germany), operated at 40 kV and 30 mA using a Ni-filtered Cu K radiation (λ = 0.15406 nm). The samples were scanned at the ambient condition over scattering 2 angles from 10° to 80° with the scanning rate of 0.02°/min. Crystallinity index (CrI) of each sample was calculated according to Segal method [24].

$$\mathrm{CrI}(\%) = \frac{I_{200} - I_{am}}{I_{200}} \times 100 \quad (1)$$

where $I_{200}$is the peak intensity at plane (200) and I_{am} is the minimum intensity at the valley between plane (200) and (110). I_{200} represents both crystalline and amorphous fractions whereas I_{am} represents only the amorphous fraction. The mean size of crystallite (D) was estimated using Debye-Scherer equation [25]

$$\mathrm{D} = \frac{k\lambda}{\beta_{1/2}\cos\theta} \quad (2)$$

where k is Scherer constant (0.91), λ is the wavelength of the radiation (λ = 0.15406 nm), $\beta_{1/2}$ is the full width at the half maximum (FWHM) of the XRD peak, and$2\theta$is the scattering angle of the peak (200).

Thermogravimetric Analysis

Thermogravimetric analysis was carried out on TA Instruments TGA Q500 to determine the thermal decomposition of fibers after each treatment. The samples of 15 20 mg were burned under temperature ranging from room temperature to 800 °C at a heating rate of 10 °C/min under a nitrogen atmosphere.

Results and Discussion

X-ray Diffraction Analysis (XRD)

Unlike hemicellulose and lignin, cellulose has a crystalline structure in nature which is formed by the hydrogen bonding and Van der Waals forces between adjacent molecules Zhang and Lynd [26]. XRD method was conducted to evaluate the crystallinity of crude fibers, cellulose, and CNCs of CHF, NFT, RH and the results were presented in Fig. 1. All the XRD patterns exhibited the characteristic diffraction peaks around $2\theta = 15.6°$ (110), 22.7° (200), and 34° (004), which confirmed that the crystal lattice type I of native cellulose [27, 28] was preserved after the chemical treatments. The gradually increasing intensity of net peaks at $2\theta = 15.6°$ and 22.7° showed that the crystallinity of material increased accordingly (Fig. 1). The crystallinity of specimens (CrI) and crystallite size were calculated in using Eq. (1) and Eq. (2), respectively. As showed in Table 1, the CrI values of NFT, CHF, and RH increased significantly when transforming from crude fibers into cellulose (43.1%, 45.4%, and 40.6–71.9%, 72.7%, and 77.5%, respectively). The result of increasing CrI value indicated that the partial elimination of hemicellulose and lignin was obtained. Furthermore, the CrI values showed a 5–7% enhancement to nearly 80% in case of CNCs sample (NFT 76.6%, CHF 79.3%, and RH 82.8%). The slightly increase of CrI after acid treatment was mainly due to the removal of amorphous domains of cellulose. During the acidic hydrolysis process, the hydronium ions penetrated the cellulose chains in these susceptible amorphous regions and accelerated the hydrolytic cleavage of the glycoside bonds, and thus released eventually the individual crystallites [29]. Moreover, the growth of crystallites size of NFT, CHF and RH in every treatment stage was attributed to the self-assembling of monocrystals to create CNCs. The improved rearrangement of CNCs results to the ability of highly ordered close packing and thus enhance the hydrogen interaction between CNCs chains, which create the high crystalline and impact structure [30]. This phenomenon resulted to the sharper diffraction peaks, and the crystallinity depends also on their origin and the isolation method. The CrI of RH (82.8%) was about 20% remarkable higher than those of other reports using different extraction methods and

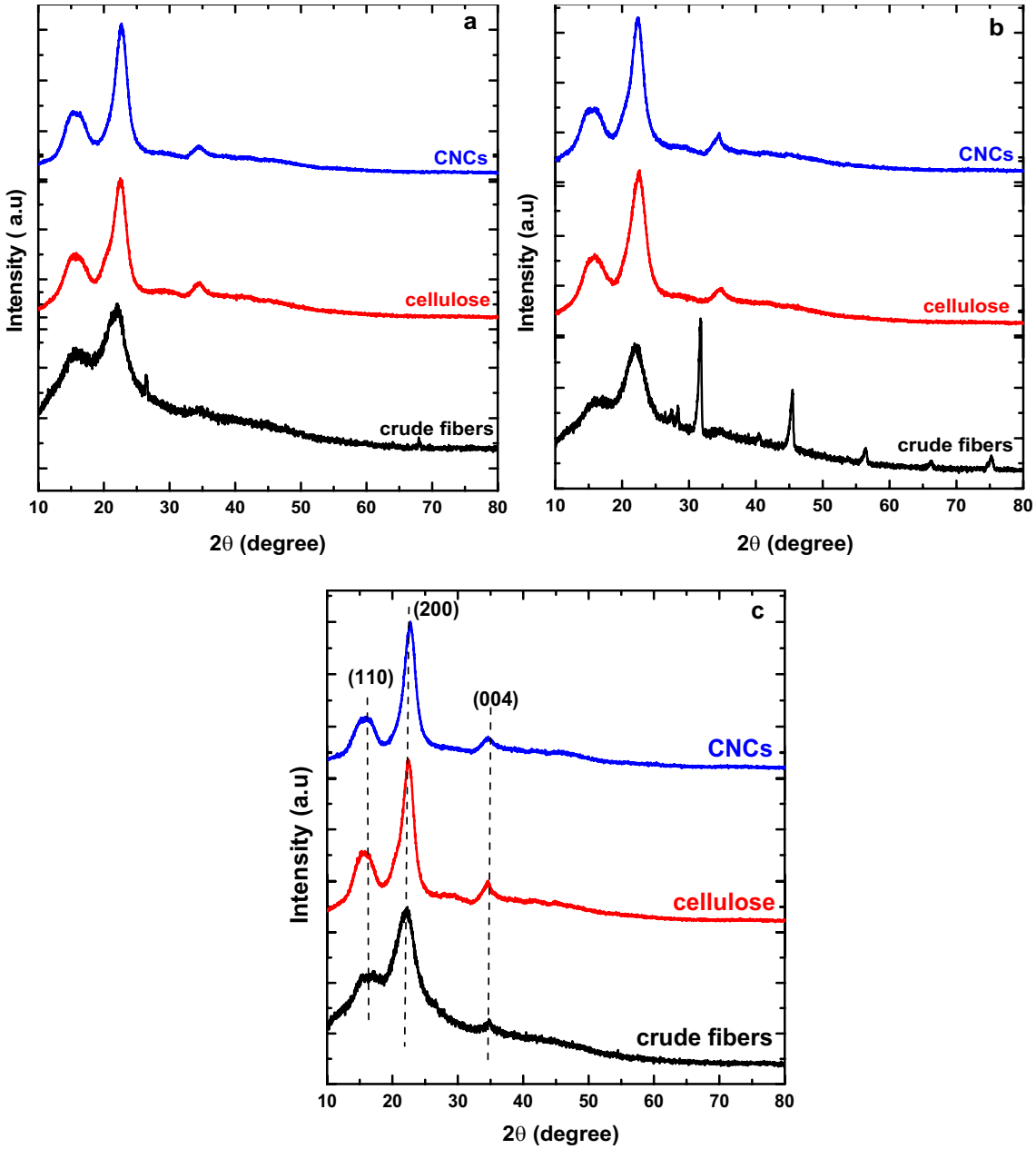

Fig. 1 XRD patterns of crude fibers, cellulose, CNCs of **a** coconut husk fiber, **b** *Nypa Fruticans* trunk and **c** rice husk

experiment conditions [31–33]. Nascimento et al. [34] have also reported a comparable CrI (75%) for CNCs isolated from CHF by chemical treatment with ultrasound attack. NFT of our study being firstly studied in literature for CNCs isolation has showed a high crystallinity (76.6%) comparable to CHF and RH which were 79.3% and 82.8%, accordingly. In brief, there is no doubt that the CrI value is affected by not only different sources of cellulose but also the chemical agents and processing method used. In addition, the crystallite size of different cellulosic materials is also consistent with the CrI values. As showed in Table 1 the crystallite size was calculated according to Scherer's equation and increased with the shape of diffraction peak.

Fourier Transformed Infrared (FT-IR) Analysis

The efficiency of each chemical treatment was evaluated by FT-IR as shown in Fig. 2. In the rice husk sample, all the spectra were characterized by a dominant O–H stretch band (3400–3200 cm^{-1}) and C–H stretch band (2900 cm^{-1}) according to the aliphatic moieties in polysaccharide while the peak near 1640 cm^{-1} was attributed to bending vibration

Table 1 Crystallinity index and crystallite size of crude fibers, cellulose, and CNCs of CHF, NFT, and RH

Fibers	Sample	Crystallinity index (%)	Crystallite size (nm)
Crude fibers	CHF	45.4	2.62
	NFT	43.1	2.48
	RH	40.6	2.88
Cellulose	CHF	72.7	2.83
	NFT	71.9	2.61
	RH	77.5	3.37
CNCs	CHF	79.3	3.35
	NFT	76.6	3.08
	RH	82.8	3.58

of O–H in water molecule Nascimento et al. [34]. In fact, it is very difficult to remove water from cellulose because of the cellulose–water interaction [35]. The vibration of C–O–C pyranose ring skeletal showed prominent absorption bands at 1076–1023 cm^{-1} Sun et al. [36]. The characteristic peaks at 1247 cm^{-1} (out of plane stretching vibration of aryl groups) and at 1516 cm^{-1} (C=C stretching of aromatic rings) correspond to the presence of lignin in crude sample. Besides, the peak at 1715 cm^{-1} was related to stretching vibration of carbonyl and acetyl groups, which is the main constituents of hemicellulose and lignin [37]. Meanwhile, the other bands at 1060 cm^{-1} and 890 cm^{-1} were associated with pure cellulose.

The FT-IR spectra of coconut husk fiber in Fig. 2a showed the presence of hemicellulose and lignin were observed by the appearance of absorbance at 1440 cm^{-1} (C=C stretch of aromatic rings of lignin), 1373 cm^{-1} (C–H asymmetric deformations), 1320 cm^{-1} (syringyl ring breathing with C–O stretching), and 1260 cm^{-1} (guaiacyl ring breathing with C=O stretching) Sun et al. [38]. The peak at 612 cm^{-1} corresponds to bending vibration of lignin rings. The prominent peak at 1730 cm^{-1} was arisen from either the acetyl and uronic ester groups of the hemicelluloses or the ester linkage of carboxylic group of the ferulic and p-coumeric acids of lignin and/or hemicelluloses [39, 38]. The typical values of cellulose at 1058 cm^{-1} and 897 cm^{-1} reflected the C–O stretching and C–H rocking vibrations of cellulose [16].

The FT-IR spectra of *Nypa Fruticans* trunk (Fig. 2b) were indicated the broad band at 3420–3340 cm^{-1}, which was associated with the hydroxyl group that normally occurred as a result of moisture absorption [38] whereas the absorbance at 2900 cm^{-1} originated from stretching vibration of C–H. The prominent peaks in the regions of 1500–1600 cm^{-1} were related to stretching of aromatic rings of lignin [38]. Also, the peak at 1731 cm^{-1} and 1251 cm^{-1} were associated with the carbonyl groups in uronic acids or acetyl groups attached to hemicellulose [40] The absorption at 1642 cm^{-1} is principally related to the absorbed water [34]. The peak at 898 cm^{-1} was attributed to the C1 group frequency or ring frequency, is characteristic of β-glycosidic linkages between the sugar units Sun et al. [36]. The absorbance at 710 cm^{-1} revealing O–H out-of-plane bending for $I_\beta$whereas the small shoulder peak at 750 cm^{-1} was associated with O–H out-of-plane bending for I_α[27]. The FT-IR results have indicated that hemicellulose, lignin, and other impurities were removed through the process of extraction of cellulose and isolation of CNCs.

Cellulose Nanocrystals Morphologies

Morphologies and size distribution of obtained CNCs were characterized by TEM. Nanosized CNCs fibers of NFT, CHF, and RH were clearly observed in the TEM images (Fig. 3) with nanorods shape, which is separating and dispersing in water. The dominant size of CNCs nanorods were ranged from 10 to 15 nm in width and less than 500 nm in length. Such dimensions are comparable to those of whiskers originating from pea hull fiber [41] and coconut husks [19]. The RH whiskers show lengths shorter than in the case of branch of mulberry [42] but RH whiskers are much thinner.

Thus, based on the combination between results of XRD and TEM images it is proved that the hydrolysis process between cellulose and sulfuric acid has occurred. The acidic protons have attacked and removed the amorphous regions in the structure of cellulose and retains its crystal structure. This leads to the CrI of CNCs higher than cellulose and the length of CNCs shorter than cellulose (as shown in TEM images).

Thermogravimetric Analysis

TGA thermograms and DTG curves (a derivative of TGA, illustrating the corresponding rate of weight loss) of crude fibers, cellulose and CNCs of NFT, CHF, and RH were shown in Fig. 4. All TGA curves presented an initial small peak in 25–150 °C range, which was mainly from free and bound water evaporation with the weight loss about 3% for CNCs, and 5% for crude fibers depending on lignocellulosic resources. The moisture content of CNCs was lower than those of crude fibers due to the dehydration of cellulose fibers during acid hydrolysis, which introduced sulfate groups at the outer surface of CNCs [43]. The crucial decomposition of crude fibers of NFT, CHF, and RH was observed at 163–231 °C with the T_{max} of 361–375 °C, leaving significant residue nearly 23–30% depending on type of biomass.

The results summarized in Table 2 showed the onset temperature of major decomposition of both cellulose fibers and CNCs, it exhibited an increment up to 245–272 °C and 170–265 °C respectively compared to that of crude fibers. The lower degradation temperature of crude fibers was

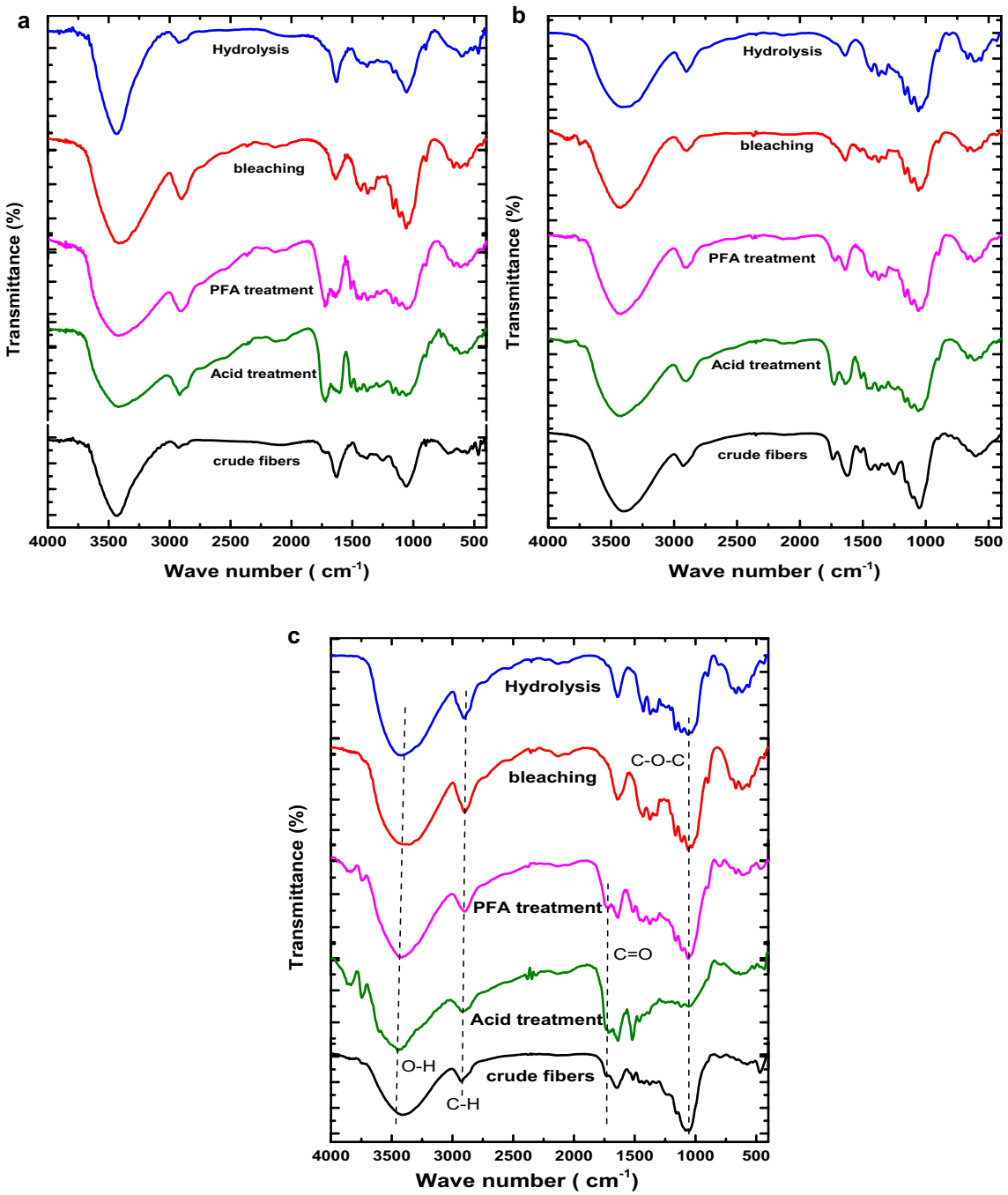

Fig. 2 FT-IR spectra of each chemical treatment of **a** coconut husk fiber, **b** *Nypa Fruticans* trunk, and **c** rice husk

attributed to the low decomposition temperature of hemicellulose, lignin, and pectin [11]. In contrary to cellulose fibers, CNCs showed a reduction in thermal stability with the onset temperature decreased remarkably (about 10–50 °C) to 190–265 °C accompanied with the decline in T_{max} of 207–322 °C, which might be associated with the faster heat transfer in CNCs due to the smaller fiber dimensions or the lower activation energy for degradation from the surface sulfate groups [43, 44]. At the final of pyrolysis process, the residue content left at 800 °C depends on lignocellulosic resources and their forms (crude fibers, cellulose, and cellulose nanocrystals). The relatively small residue in cellulose fibers implied the partial removal of hemicellulose and lignin from the fibers. The higher char of CNCs compared to cellulose fibers was ascribed to the flame retarding of sulfate ester groups introduced in acid hydrolysis [44]. The similar

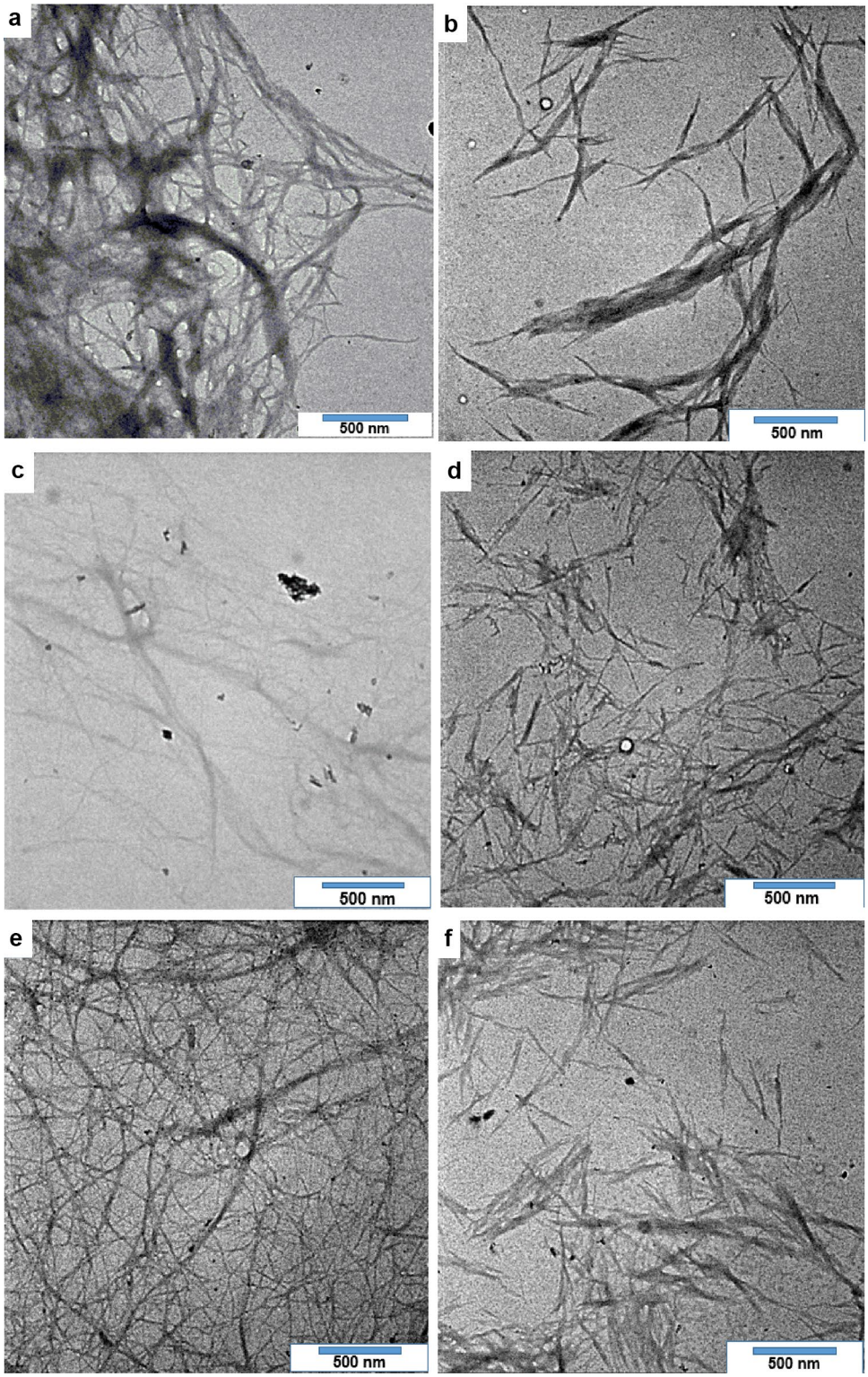

Fig. 3 TEM images of cellulose (**a**, **c**, **e**) and CNC whiskers (**b**, **d**, **f**) of *Nypa Fruticans* trunk, coconut husk fiber and rice husk

pyrolysis behavior was also observed in CNCs extracted from garlic straw [45], wheat straw, wood, bamboo, and flax [11]. In brief, the different final residues at 800 °C were not only influenced by the source of biomass but also by the condition of CNCs isolation.

Conclusion

CNCs were successfully isolated from three different by-product resources, i.e., *Nypa Fruticans* trunk (NFT), coconut husk fiber (CHF), and rice husk (RH) by using chemical

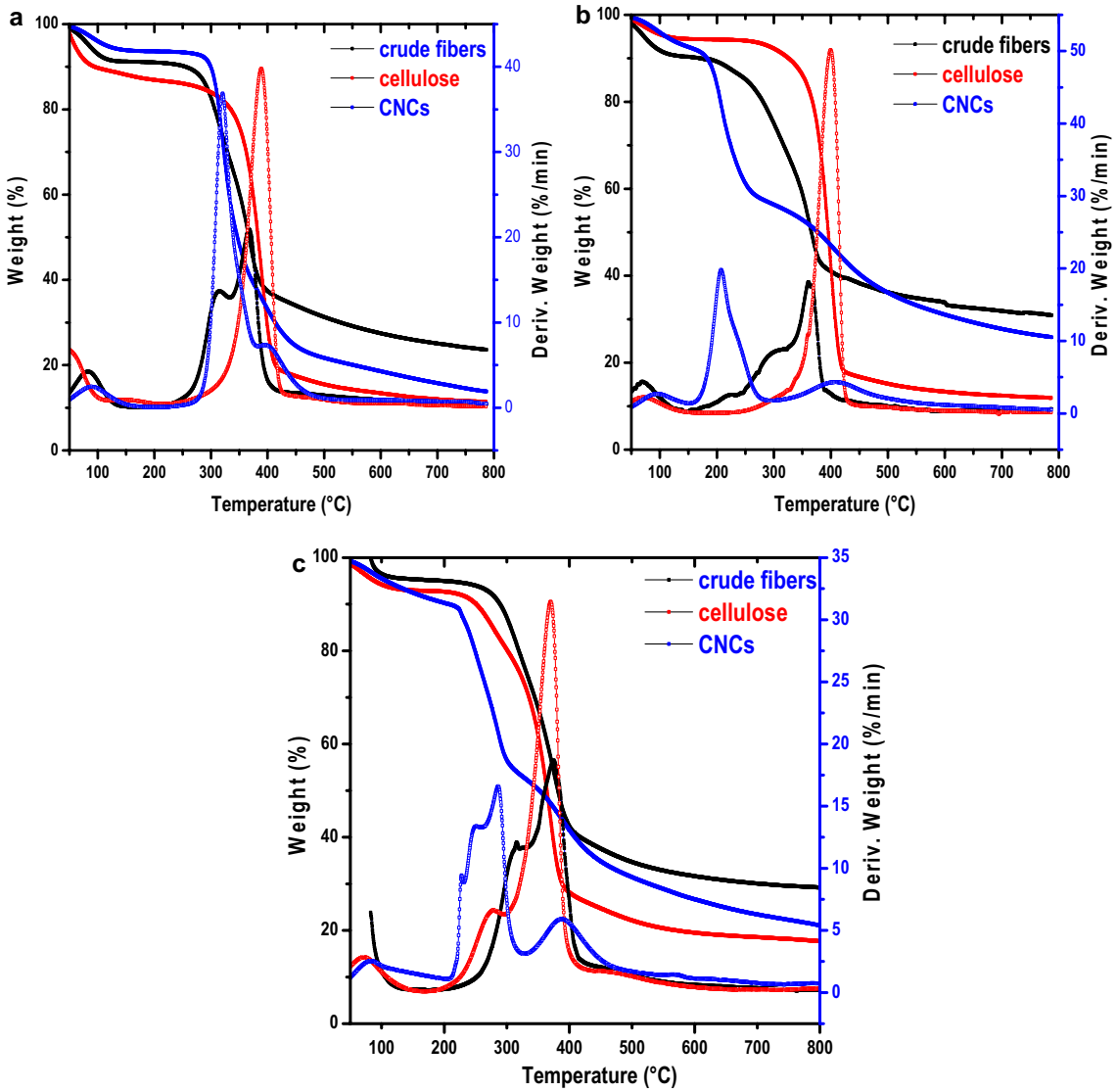

Fig. 4 TGA and DTG curves of crude fibers, cellulose, CNCs of **a** coconut husk fiber, **b** *Nypa Fruticans* trunk, and **c** rice husk

Table 2 Thermogravimetric analysis of CHF, NFT, and RH at different stages

Fibers	Sample	Decomposition Temp.		Char at 800 °C
		Onset/end Temp.(°C)	T_{max}	
Crude fibers	CHF	231–437	368	23.7
	NFT	163–434	361	30.9
	RH	222–415	375	29.2
Cellulose	CHF	272–447	389	11.4
	NFT	246–457	400	11.9
	RH	245–430	370	17.7
CNCs	CHF	265–494	322	13.9
	NFT	190–694	207	25.9
	RH	208–477	286	21.1

treatments with high crystallinity of 76.6%, 79.3%, and 82.8% for NFT, CHF, and RH respectively. Also, the yields of nanocellulose synthesis was determinated at about 30–40% wt depending on the resource materials (NFT: 38–40%; CHF: 30–32% và RH: 35–37%). In other hand, the sulfuric acid hydrolysis contributed to protect CNCs from pyrolysis by the char of sulfate ester groups which are outer of CNCs surface acted as a flame retardant. TEM images confirmed that the synthesized nanocellulose fibers diameter was in the range of 10–15 nm. Thermogravimetric analysis showed improved thermal stability for nanocellulose fibers, which makes them suitable in the manufacturing of bio-nanocomposites for various applications such as functional paper, versatile support for preparing metal/oxide metal nanoparticles, membrane filter [46]. This study demonstrates that with the dimensions at nanoscale, cellulose whiskers

isolated from NFT, CHF, and RH by acid hydrolysis promise potential resources for the nano-natural material suitable for further high value-added applications (optoelectronics, packaging, mechanically reinforced polymer composites, tissue scaffolds, environmental remediation, etc.) from agricultural wastes/by-products and also contribute to prevent environment pollution by these biomass sources.

Acknowledgements This research is funded by Vietnam National University HoChiMinh City (VNU-HCM) under Grant Number of *562-2018-18-01*. Authors are grateful for this financial support.

References

1 Habibi Y, Lucia LA, Rojas OJ (2010) Cellulose nanocrystals: chemistry, self-assembly, and applications. Chem Rev 110(6):3479–3500
2 Moon RJ, Martini A, Nairn J, Simonsen J, Youngblood J (2011) Cellulose nanomaterials review: structure, properties and nanocomposites. Chem Soc Rev 40(7):3941–3994
3 Fitri R, Lee G, Rawal A, Hutomo T, Stenzel M, Arcot J (2016) Nanocellulose characteristics from the inner and outer layer of banana pseudo-stem prepared by TEMPO-mediated oxidation. Cellulose 23(5):3023–3037
4 Hastuti N, Kanomata K, Kitaoka T (2018) Hydrochloric Acid hydrolysis of pulps from oil palm empty fruit bunches to produce cellulose nanocrystals. J Polym Environ 26(9):3698–3709
5 Sun B, Zhang M, Hou Q, Liu R, Wu T, Si C (2016) Further characterization of cellulose nanocrystal (CNC) preparation from sulfuric acid hydrolysis of cotton fibers. Cellulose 23(1):439–450
6 Baati R, Mabrouk AB, Magnin A, Boufi S (2018) CNFs from twin screw extrusion and high pressure homogenization: a comparative study. Carbohydr Polym 195:321–328. https://doi.org/10.1016/j.carbpol.2018.04.104
7 Panyasiri P, Yingkamhaeng N, Lam NT, Sukyai P (2018) Extraction of cellulose nanofibrils from amylase-treated cassava bagasse using high-pressure homogenization. Cellulose 25(3):1757–1768. https://doi.org/10.1007/s10570-018-1686-6
8 Chen X-Q, Deng X-Y, Shen W-H, Jia M-Y (2018) Preparation and characterization of the spherical nanosized cellulose by the enzymatic hydrolysis of pulp fibers. Carbohydr Polym 181:879–884. https://doi.org/10.1016/j.carbpol.2017.11.064
9 Liu X, Jiang Y, Qin C, Yang S, Song X, Wang S, Li K (2018) Enzyme-assisted mechanical grinding for cellulose nanofibers from bagasse: energy consumption and nanofiber characteristics. Cellulose 25(12):7065–7078. https://doi.org/10.1007/s10570-018-2071-1
10 Zhang K, Zhang Y, Yan D, Zhang C, Nie S (2018) Enzyme-assisted mechanical production of cellulose nanofibrils: thermal stability. Cellulose 25(9):5049–5061. https://doi.org/10.1007/s10570-018-1928-7
11 Chen W, Yu H, Liu Y, Hai Y, Zhang M, Chen P (2011) Isolation and characterization of cellulose nanofibers from four plant cellulose fibers using a chemical-ultrasonic process. Cellulose 18(2):433–442. https://doi.org/10.1007/s10570-011-9497-z
12 Hsieh Y-L (2013) Cellulose nanocrystals and self-assembled nanostructures from cotton, rice straw and grape skin: a source perspective. J Mater Sci 48(22):7837–7846
13 Silvério HA, Neto WPF, Dantas NO, Pasquini D (2013) Extraction and characterization of cellulose nanocrystals from corncob for application as reinforcing agent in nanocomposites. Ind Crops Prod 44:427–436
14 Li F, Mascheroni E, Piergiovanni L (2015) The potential of nanocellulose in the packaging field: a review. Packag Technol Sci 28(6):475–508
15 Ashori A, Nourbakhsh A (2010) Bio-based composites from waste agricultural residues. Waste Manag 30(4):680–684
16 Alemdar A, Sain M (2008) Isolation and characterization of nanofibers from agricultural residues: wheat straw and soy hulls. Biores Technol 99(6):1664–1671. https://doi.org/10.1016/j.biortech.2007.04.029
17 Li J, Wei X, Wang Q, Chen J, Chang G, Kong L, Liu Y (2012) Homogeneous isolation of nanocellulose from sugarcane bagasse by high pressure homogenization. Carbohydr Polym 90(4):1609–1613
18 Reddy JP, Rhim J-W (2014) Isolation and characterization of cellulose nanocrystals from garlic skin. Mater Lett 129:20–23
19 Rosa M, Medeiros E, Malmonge J, Gregorski K, Wood D, Mattoso L, Imam S (2010) Cellulose nanowhiskers from coconut husk fibers: Effect of preparation conditions on their thermal and morphological behavior. Carbohydr Polym 81(1):83–92
20 Zuluaga R, Putaux JL, Cruz J, Vélez J, Mondragon I, Gañán P (2009) Cellulose microfibrils from banana rachis: effect of alkaline treatmentson structural and morphological features. Carbohydr Polym 76(1):51–59
21 John MJ, Thomas S (2008) Biofibres and biocomposites. Carbohydr Polym 71(3):343–364
22 Thuc CNH, Thuc HH (2013) Synthesis of silica nanoparticles from Vietnamese rice husk by sol–gel method. Nanoscale Res Lett 8(1):58
23 Tong KT, Vinai R, Soutsos MN (2018) Use of Vietnamese rice husk ash for the production of sodium silicate as the activator for alkali-activated binders. J Clean Prod 201:272–286. https://doi.org/10.1016/j.jclepro.2018.08.025
24 Segal L, Creely J, Jr M, Conrad C (1959) An empirical method for estimating the degree of crystallinity of native cellulose using the X-ray diffractometer. Text Res J 29(10):786–794
25 Elazzouzi-Hafraoui S, Nishiyama Y, Putaux J-L, Heux L, Dubreuil F, Rochas C (2007) The shape and size distribution of crystalline nanoparticles prepared by acid hydrolysis of native cellulose. Biomacromol 9(1):57–65
26 Zhang YHP, Lynd LR (2004) Toward an aggregated understanding of enzymatic hydrolysis of cellulose: noncomplexed cellulase systems. Biotechnol Bioeng 88(7):797–824
27 Lu P, Hsieh Y-L (2010) Preparation and properties of cellulose nanocrystals: Rods, spheres, and network. Carbohydr Polym 82(2):329–336. https://doi.org/10.1016/j.carbpol.2010.04.073
28 Sugiyama J, Vuong R, Chanzy H (1991) Electron diffraction study on the two crystalline phases occurring in native cellulose from an algal cell wall. Macromolecules 24(14):4168–4175
29 de Souza Lima MM, Borsali R (2004) Rodlike cellulose microcrystals: structure, properties, and applications. Macromol Rapid Commun 25(7):771–787
30 Lu P, Hsieh Y-L (2012) Preparation and characterization of cellulose nanocrystals from rice straw. Carbohydr Polym 87(1):564–573
31 Khandanlou R, Ngoh GC, Chong WT (2016) Feasibility study and structural analysis of cellulose isolated from rice husk: microwave irradiation, optimization, and treatment process scheme. BioResources 11(3):5751–5766
32 Nascimento P, Marim R, Carvalho G, MaliS (2016) Nanocellulose produced from rice hulls and its effect on the properties of biodegradable starch films. Mater Res 19(1):167–174
33 Rosa SM, Rehman N, de Miranda MIG, Nachtigall SM, Bica CI (2012) Chlorine-free extraction of cellulose from rice husk and whisker isolation. Carbohydr Polym 87(2):1131–1138
34 Nascimento DMd, Dias AF, Araújo Junior CP, de Freitas Rosa M, Morais JP, de Figueirêdo MC (2016) A comprehensive approach

for obtaining cellulose nanocrystal from coconut fiber. Part II: environmental assessment of technological pathways. Ind Crops Prod 93:58–65. https://doi.org/10.1016/j.indcrop.2016.02.063
35 Abraham E, Deepa B, Pothan L, Jacob M, Thomas S, Cvelbar U, Anandjiwala R (2011) Extraction of nanocellulose fibrils from lignocellulosic fibres: a novel approach. Carbohydr Polym 86(4):1468–1475
36 Sun X-F, Sun R-C, Su Y, Sun J-X (2004) Comparative study of crude and purified cellulose from wheat straw. J Agric Food Chem 52(4):839–847
37 Qazanfarzadeh Z, Kadivar M (2016) Properties of whey protein isolate nanocomposite films reinforced with nanocellulose isolated from oat husk. Int J Biol Macromol 91:1134–1140
38 Sun X-F, Sun R, Fowler P, Baird MS (2005) Extraction and characterization of original lignin and hemicelluloses from wheat straw. J Agric Food Chem 53(4):860–870
39 Sain M, Panthapulakkal S (2006) Bioprocess preparation of wheat straw fibers and their characterization. Ind Crops Prod 23(1):1–8
40 Sun X-F, Jing Z, Fowler P, Wu Y, Rajaratnam M (2011) Structural characterization and isolation of lignin and hemicelluloses from barley straw. Ind Crops Prod 33(3):588–598
41 Chen Y, Liu C, Chang PR, Cao X, Anderson DP (2009) Bionanocomposites based on pea starch and cellulose nanowhiskers hydrolyzed from pea hull fibre: effect of hydrolysis time. Carbohydr Polym 76(4):607–615. https://doi.org/10.1016/j.carbpol.2008.11.030
42 Li R, Fei J, Cai Y, Li Y, Feng J, Yao J (2009) Cellulose whiskers extracted from mulberry: a novel biomass production. Carbohydr Polym 76(1):94–99
43 Roman M, Winter WT (2004) Effect of sulfate groups from sulfuric acid hydrolysis on the thermal degradation behavior of bacterial cellulose. Biomacromolecules 5(5):1671–1677
44 Jiang F, Hsieh Y-L (2013) Chemically and mechanically isolated nanocellulose and their self-assembled structures. Carbohydr Polym 95(1):32–40
45 Kallel F, Bettaieb F, Khiari R, García A, Bras J, Chaabouni SE (2016) Isolation and structural characterization of cellulose nanocrystals extracted from garlic straw residues. Ind Crops Prod 87:287–296
46 Islam MS, Chen L, Sisler J, Tam KC (2018) Cellulose nanocrystal (CNC)–inorganic hybrid systems: synthesis, properties and applications. J Mater Chem B 6(6):864–883. https://doi.org/10.1039/C7TB03016A